Figure 21. Slab from PAC 3, New Creek Formation, St. Clairsville.

The top of the cycle corresponds to the top of the slab (note eroded brachiopod shell). Chert is mostly in the middle zone, which contains abundant coarse fossil particles and organic matter. The silicification is irregular, though confined to a zone. This cherty zone is bounded by micrite below and argillaceous micrite above. The silicification pattern of the brachiopod shell in upper part is reminiscent of opaline spherules. The scale is in millimeters.

or saturation levels, which are dependent on various sedimentologic and geochemical factors (see Chapter III). The top of PAC 1 contains chert as a thick bed at Limestoneville, as nodules at Tyrone and associated with concretions, both siliceous and calcareous, at Allegheny Furnace. Hence the distribution of silicification patterns in the lower New Creek Formation are controlled by stratigraphic processes, but the exact location of chert is dependent on local sedimentological or mineralogical conditions producing suitable microenvironment.

Upper New Creek Formation

The more argillaceous, thinner-bedded upper New Creek Formation varies from 2.5 to 5 ft (0.76 to 1.52 m) in thickness. The three cycles comprising the upper New Creek are thin, averaging 1.2 ft (0.37 m) in thickness. Cycle boundaries in this interval are characterized by thin clay partings and/or shell lags. Lateral variation in facies is more noticeable in this section than in the lower New Creek Formation. For example, Tyrone is the shallowest location as indicated by the presence of cryptalgal laminites at the top of the formation. In contrast, at Limestoneville abundant chert and finer calcarenite are the deepest facies in the interval (Figures 18 and 20). South and east of Tyrone upper New Creek facies are totally subtidal, consisting largely of fine-grained, argillaceous calcarenite. Numbers of cycles and cycle thickness remain same throughout the study are. Chert occurs as discontinuous lenses and as beds at cycle boundaries.

Topographic lows and highs may have caused local variations in the patterns observed. For example, there is a distinct intra-cycle surface in PAC 5 at Hollidaysburg

a) b)

Figure 22. Slabs from PAC 2, lower New Creek Fmn, Canoe Creek Quarry and Tyrone.

On the left is a bed of chertified grainstone from Canoe Creek Quarry (a). On the right is a non-cherty bed, at the same stratigraphic horizon, the top of PAC 2, at Tyrone (b). The structure and textures are similar in the two samples; grainstone, which is composed of small fossil particles, is overlain by a finer-grained cap. Hence, lithology by itself cannot be the sole determining factor of silicification. Supply of silica at a site may vary; organic matter content may differ; the overlying sediments may affect preservation of silica and degree of silicification. See thin-section of the Tyrone slab, Figure 23.

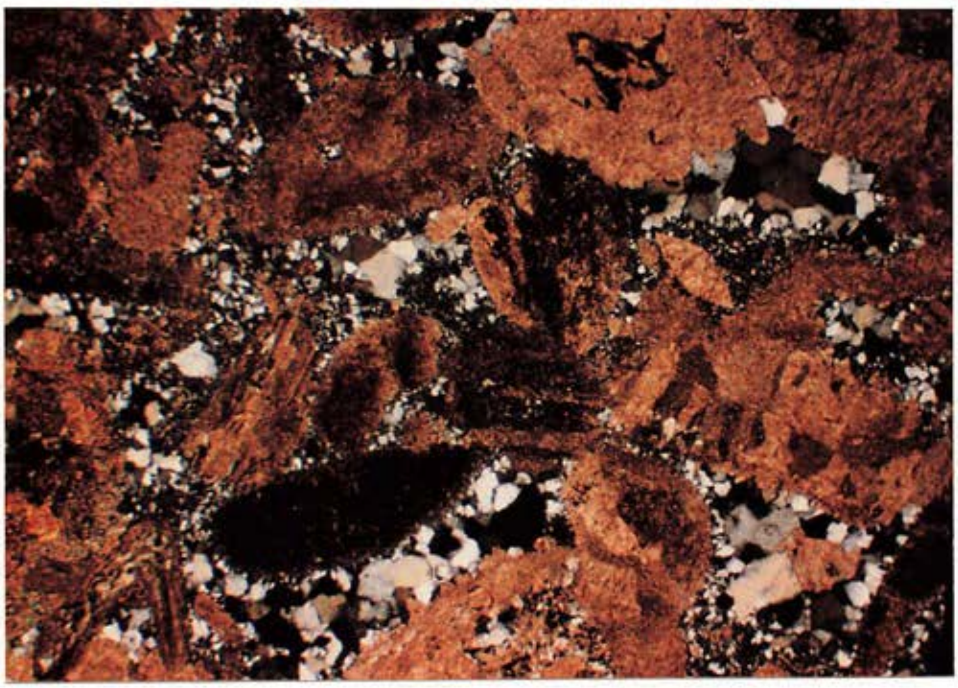

Figure 23. Thin-section from the top of PAC 2, lower New Creek Formation, Tyrone.

The grainstone of PAC 2 is silicified only in the pore spaces. Silica is finer-grained surrounding the fossil particles, but macrocrystalline throughout, and thus not chert. Lack of contact between the fossil particles indicates early cementation, whether the primary cementation was silica or silica-replaced calcite. Macrocrystalline silica crystallizes from solution with low concentration of silica. Width of photomicrograph is 3.6 mm.

and Altoona Bypass. At Hollidaysburg, the lower portion of the cycle becomes more argillaceous toward this surface; the bottom of the upper part is characterized by a shell lag. At Altoona Bypass there is a distinct surface denoted by a very thin clayey (scaly) surface. This intra-cycle surface is not correlative with any other locality, and yet at the two localities mentioned the change in lithology across the boundary would indicate a possible PAC boundary. Because of lack of correlation, the surface is interpreted to be scoured by a storm and hence an autogenic feature; the storm affected only certain parts of the basin, thus reflecting topographic or basinal variations.

Chert occurs most persistently associated with the PAC-boundary on top of PAC 6 and less persistently at other cycle boundaries. This prominent chert below the New Creek-Corriganville boundary is the most important chert because of its thickness and continuity (Figures 10 and 11). At the lesser boundaries (6th-order instead of 5th-order), the character of chert is often nodular or intermittent, the occurrence corresponding to lithology (*e.g.* fossil particles). This observation would suggest that the primary control is by stratigraphic processes and secondary control by sedimentologic processes, which produced different host lithologies.

The chert in PAC 6 is positioned often below the cycle surface and associated with burrowing activity in addition to fossil accumulation (Figures 10, 24 and 25), the morphology of chert being controlled by inhomogeneities in sediments, and perhaps, by mechanical transportation of siliceous matter into the sediments by burrowing. The 6th-order cycle boundary between PACs 4 and 5 contains chert associated with fossil lag at four localities, Cessna, Hollidaysburg, Allegheny Furnace and Limestoneville, out of the seven localities studied. This thick continuous chert bed is interpreted to be linked to the major deepening event, which perhaps indicates increased time of non -deposition, at the base of the Corriganville Formation.

Cycles and Chert in the Corriganville Formation

General Characterictics

The Corriganville Formation, which averages 12.4 ft (3.78 m) in thickness, consists of nine laterally correlative cycles (Figure 9). In contrast to cycles in the New Creek Formation, Corriganville cycles have well developed high-stand and low-stand portions. A typical Corriganville cycle is a thinly bedded unit of 1.4 ft (0.43 m), which is constructed of a finer-grained high-stand portion and an abundantly fossiliferous coarser-grained low-stand portion. As in the New Creek Formation, the character of the lower Corriganville cycles differs from that of the upper Corriganville cycles. The PACs in the lower Corriganville have well developed high- and low-stand parts, the high-stand part being calcareous shale and the low-stand fine- to medium-grained calcarenite with abundance of brachiopods and bryozons. The PACs are thinner in the upper part of the Corriganville Formation, and they tend to be finer-grained, consisting of chert-rich calcareous mudstones and shales. The high-stand portion of each cycle is proportionally thinner or nearly absent.

The general pattern of chert occurrence in the Corriganville Formation follows a distribution restricted to high-stand portions of the cycles and surfaces representing depositional hiatus, at cycle boundaries and sea-level fall surfaces. Chert tends to occur more as continuous, laterally correlative beds than in the New Creek Formation. Chert occurs in limited quantities in the lower Corriganville Formation, where it is found below cycle boundaries or associated with shell hash internal to a cycle. In the upper Corriganville Formation chert is found particularly concentrated in the high-stand portion of PAC 6, and thereafter associated with PAC boundaries and sea-level fall surface or a shell lag in association with a stratigraphic surfaces. Hence chert occurs in a much more clearly defined pattern in the Corriganville Formation than in the New Creek Formation.

Lower Corriganville Formation

The three lower Corriganville cycles are composed of high-stand parts of shale and nodular micrite and fine-grained calcarenitic low-stands. The average thickness of the interval is 4.2 ft (1.28 m), the thickness ranging from 3 to 5 ft (0.91 to 1.52 m). The average cycle thickness is 1.4 ft (0.43 m). PAC 1, approximately 1 ft (.30 m) thick, is composed of shale/nodular limestone at its base, thicker calcarenite beds in the upper portion and a chert bed at its top (Figure 26). This PAC is almost devoid of fossils. PACs 2 and 3 were described as a single unit in previous interpretations (Eskel and Goodwin, 1994; Orzechowski, 1995). However, in this study a study-area wide correlative surface associated with a vertical lithological change indicates a PAC boundary within this interval. This lithological change is accentuated by a fossil lag and a more argillaceous surface, above which there often occurs a nodular zone, corresponding to a poorly developed high-stand part. At one locality (Figure 26), there is a thin bentonite layer at sea-level-fall surface of PAC 2. The top portion of PAC 3 is richly and diversely fossiliferous; fossils include brachiopods, crinoid stems, trilobites, bryozoans and graptolites.

The lower Corriganville contains less continuous chert than does the upper Corriganville. High-stand part of PAC 1 contains chert only at Hollidaysburg and Altoona Bypass, where it forms a 2-4" (5.08-10.16 cm) thick chertified laminated micrite bed (Figure 26). At Tyrone, there are dolomite nodules 0.20-0.23" (6-7 cm) below the cycle boundary both in the high-stand part of PACs 1 and 2. There is chert on the top of PAC 3 in the northernmost four of the seven localities (Figure 27). At Limestoneville this 0.5 ft (0.15 m) thick chert bed occupies most of the high-stand part of the cycle. The low-stand part is thinner, consisting mostly of bioturbated shale. At Tyrone, this same stratigraphic horizon is characterized by a 0.07-0.91" (2-3 cm) thick chert bed on top of the high-stand part of the cycle, which contains bioturbated, fine-grained calcarenite (Figures 18 and 28).

<u>Upper Corriganville Formation</u>

The average thickness of the upper Corriganville is 8.0 ft (2.44 m), with a range from 7 to 9 ft (2.13 to 2.74 m). This interval consists of six laterally correlative cycles averaging 1.3 ft (0.40 m) in thickness (Figure 29). The cycles consist of distinct high-stand and low-stand portions, which, depending on location, consist of variations of shale-limestone, chert-limestone or nodular/argillaceous-calcarenite. The general grain-size of this unit is finer than in the lower Corriganville, and the typical fauna is bryozoan stems,

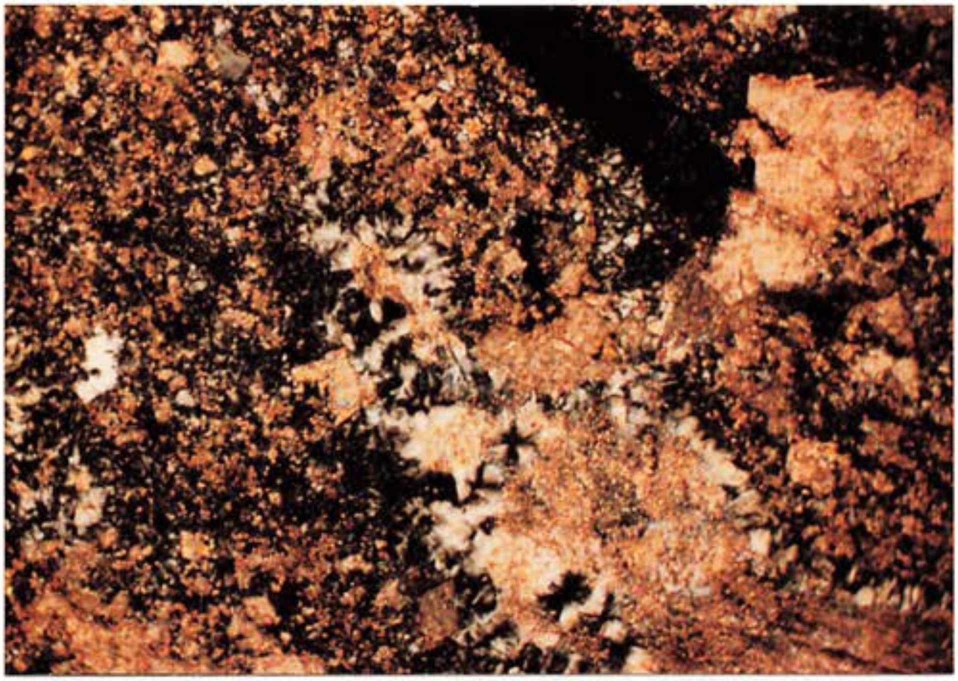

Figure 24. Thin-section from PAC 6, upper New Creek Formation, Hollidaysburg.

This thin-section is from the bedded high-stand portion of PAC 6. Most of the rock is composed of fine grains of carbonate and silica in intimate association attesting a partial silicification pattern; no zonation is observed. Some chalcedony spheroids are associated with fossils or voids. Width of photomicrograph is 3.6 mm.

Figure 25. Slab from the top of PAC 6, upper New Creek Formation, Altoona Bypass.

The morphology of this chert is controlled by bioturbation. The light grey bulbous forms are chert; the light-brownish areas are limestone. Many fossils are seen as nearly white replacements or they are surrounded by light-colored haloes. The darker brown is organic matter.

Figure 26. PAC 1, Corriganville Formation, Hollidaysburg.

The 12" scale rests on the New Creek-Corriganville formational boundary. The top of PAC 1 is above the dark blue-gray chert bed. Above this bed is the high-stand portion of PAC 2, which extends to the shale-calcarenite boundary.

brachiopods, crinoid stems and graptolites. There is increased bioturbation toward the top of the interval as well as toward the top of an individual cycle.

The general pattern of the cycles in the upper Corriganville is entirely correlative throughout the study area (Figures 12-19). PAC 4 is a typical Corriganville PAC with a shaly high-stand and calcarenitic low-stand parts (Figure 29). PAC 5 is a very thin cycle, composed of fine calcarenite and an irregular chert bed at the top of the cycle. PAC 6 is unique in its pattern of laterally traceable features; the high-stand part is composed of shale and thin beds of chert, the low-stand portion of fine calcarenite. This sea-level-fall surface contains a distinct, laterally continuous chert bed (Figure 31). The low-stand parts of PAC 6 and PAC 7 form a distinctive two-bed unit recognizable throughout the study area; the cycle boundary between them is characterized by a fossil layer and clay seam. Minor nodular chert is associated with this surface. The base of PAC 8 contains a distinctively thick chert bed with a characteristic blueish hue (Figures 32 and 33). PAC 9 has a thin shaly high-stand part, is usually devoid of chert and is extensively bioturbated.

The major concentration of chert in the upper Corriganville Formation occurs within the PAC 5 through PAC 8 interval. Chert connected with cycle boundaries 5-6 and 7-8 are thick, and even in outcrop have a blueish hue (*e.g.* Figures 26, 29, and 30). Chert in this interval seems to be more completely silicified than chert in the New Creek Formation (Figure 34), and this and the abundance of chalcedonic silica (Figures 35 and 36) causing the blue color. The coarser, more fossiliferous, and probably more permeable portions of beds, are the most completely silicified (Figure 37).

Figure 27. Upper Corriganville Formation, Limestoneville.

The lower Corriganville-upper Corriganville boundary is at the top of the thick prominent chert bed behind the 12" scale. The chert bed is the low-stand portion of PAC 3; the high-stand portion is the 2.5" thick calcareous mudstone bed. The top of PAC 4 is the surface at 1.5' on the measuring stick. PAC 5 is nearly 2.5 ft thick, composed of a shaly high-stand part and a calcarenitic low-stand part.

Figure 28. PACs 3, 4 and 5, Corriganville Formation, Tyrone.

The measuring stick rests on the PAC 3-4 boundary. The top of PAC 3 is visible; there is a thin chert layer immediately below the stick. The interval of shaley, nodular calcareous mudstone forms the high-stand portion of PAC 4. The calcarenite bed is the low-stand part of PAC 4.

Figure 29. Upper Corriganville Formation, Altoona Bypass.

The measuring stick rests on top of PAC 3. The Corriganville-Mandata boundary is above the last competent calcarenite bed in the right hand corner. PAC 4, which is the first upper Corriganville PAC, consists of 6" of high-stand shale and nodular micrite overlain by 18" of massive calcarenite; this is also the beginning of the upper Corriganville Formation. PAC 5 is about 6" thick, behind the 2' and 2.5' marker in the measuring stick. The thin chert beds and calcareous mudstone of the high-stand part of PAC 6 are between the 2.5' marker and the 12" scale (at the sea-level-fall surface) . Note the thick, blue-gray bed of chert below the sea-level fall surface. The top of PAC 6 coinsides with the top of the measuring stick. PAC 9 is composed of a distinct high-stand part, a thin boudinaged layer, and a low-stand part, which is bioturbated, medium-grained calcarenite.

Figure 30. PACs 3, 4, 5 and 6, Corriganville Formation, Tyrone.

The measuring stick points to the PAC 4-5 boundary. PAC 5 is a thin cycle consisting of an irregular basal chert bed (dark blue), and a six-inch bed of medium-grained calcarenite. The high-stand portion of PAC 6 is mostly behind the tree root; it consists of thin-bedded chert, calcareous mudstone and calcarenite.

Figure 31. Slab from PAC 6, upper Corriganville Formation, St. Clairsville.

This slab is from the basal bed of the cycle. The lower part of the slab is composed of a layer rich in organic matter and a few fossils. Most of these fossils are silicified. Above this darker zone is a well chertified layer, in which most of the fossils have been obliterated. Except for a few preferentially silicified fossils, the calcareous mudstone is not silicified. Width of photograph is 4.5 cm.

Figure 32. Slab from PAC 8[1], upper Corriganville Formation, Hollidaysburg.

This slab contains a potential PAC 7-8 boundary below the white and blue zone of chert at the dark line. Below this line, chert has replaced micrite, of which some is visible in the dotted light brown clump. On the left and above the clump, sponge spicules are preserved in the silicified matrix. Above the PAC boundary, white to blue chert has replaced a coarse fossil layer. Most of the fossils are seen as haloes (ghosts), some of which are only residual matter, *e.g.* iron, left from the original fossil. A thin-section of this sample is shown in Figure 35. Scale is in mm.

Figure 33. Slab from PAC 8^2, the upper Corriganville Formation, Hollidaysburg.

This is the upper part of the slab described in Figure 34. The original lithology is still discernible as outlines of fossils and carbonate grains, though there is no internal detail visible. Between the fossil particles and carbonate grains, chert is white and opaque, probably corresponding to chalcedonic fill of voids or pore spaces. The upper portion of the chertified graded bed is fine-grained and laminated. The bed is capped by laminated purely calcareous layer. A thin-section from the middle part of this slab is shown in Figure 36. Width of photograph is 4.5 cm.

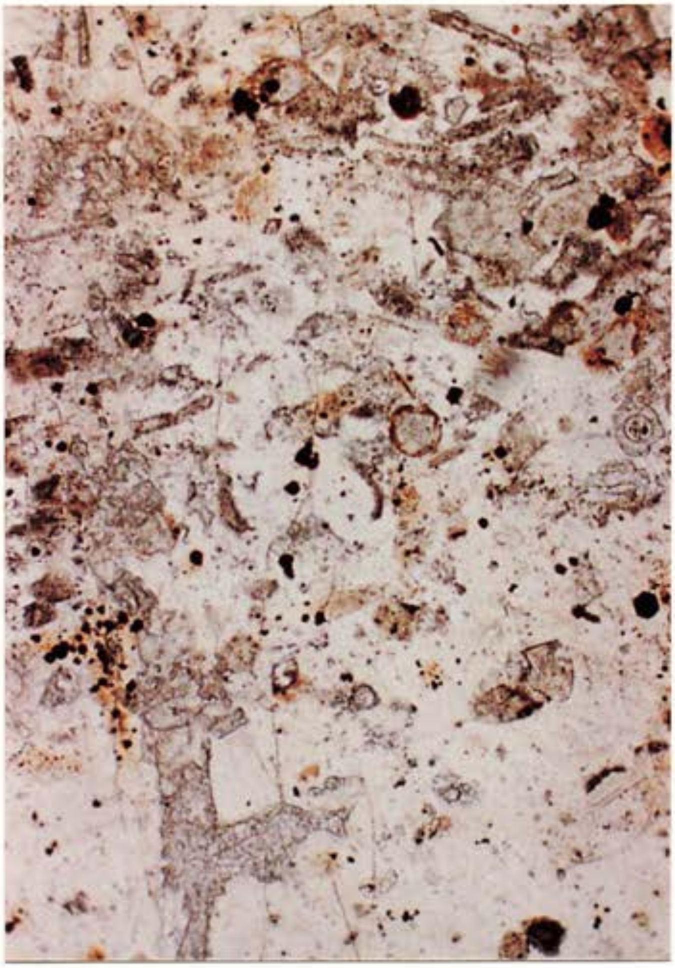

Figure 34. Thin-section from PAC 8, Corriganville Formation, Altoona Bypass.

This is a plane-polarized view of a well silicified, graded Corriganville chert on the edge of a fossiliferous zone. Some fossil matter is corroded, some of it is seen as brown staining, while some outlines are fairly discernible; most of the thin-section is nearly featureless matrix. The black spots are pyrite. Carbonate rhombohedra are visible especially in the upper half of the thin-section. The appearance of this graded bed is nearly identical to the bed from PAC 8, Hollidaysburg (see Fig. 32, 33, 35 and 36). Width of photomicrograph is 2.5 mm.

Figure 35. Thin-section from PAC 8[1], Corriganville Formation, Hollidaysburg.

The lower half of this slab, PAC 8, Corriganville Formation, is white and blue in handsample. The dominant chert fabric is chalcedony spherules, as seen in the radiating structure of the fibrous quartz. The yellow-brown band is a calcite vein. In the lower part of the photograph, zebraic chalcedony extents through half of the field of view. Zebraic chalcedony is composed of fibrous chalcedony, in which the fibers twist along the crystallographic a-axis; the variation in the orientation of the c-axis causes the extinction flow through the fibers in an undulatory fashion. Width of photomicrograph is 1.2 mm.

Figure 36. Thin-section from PAC 8², Corriganville Formation, Hollidaysburg.

This thin-section is from the same slab as the previous thin-section, but higher in the sample. Carbonate rhombs are well formed. Pore spaces are filled by spherular chalcedony; where two spherules started growing at the same time, the fibers meet forming a knife-sharp surface. Some of the original carbonate fabric is seen as the yellow fragments. Fossils are recognized by the arrangement and size of microcrystalline silica; for example, there is an outline of a fossil in the middle left of the photograph. Width of photomicrograph is 3.6 mm.

Figure 37. Thin-section from PAC 5, Corriganville Formation, Allegheny Furnace.

This thin-section is of the top of fine-grained chert-bed abd the base of a calcarenitic tempestite. The bedding plane is characterized by abundant pyrite, which is seen as black spots throughout the chert immediately below the boundary. At the boundary (in the middle of the photograph) is a part of a brachiopod shell, which has been replaced by larger grains of silica and carbonate grains, which cut across the shell-matrix boundary, indicating a later phase of calcitization. The lower part is nearly fully silicified chert as seen by pinpoint, black silica, which contrasts with the larger, chalcedonic grains of the brachiopod shell. The upper part of the view is dominated by calcareous fossil particles (yellow-brown) of the tempestite. Width of photomicrograph is 2.5 mm.

Milankovitch Hierarchy

The presence of six allocycles in the New Creek Formation and nine in the Corriganville requires a modification of Orzechowski's interpretation of each formation as a single 5^{th}-order (100 ky) sequence. Within a process-determined hierarchy of allocycles (Figure 6), there are a maximum of five precessional cycles within one short eccentricity 5^{th}-order and four 5^{th}-order sequences within a long eccentricity 4^{th}-order sequence, the 4^{th}-order sequence being of 400 ky duration. Orzechowski (1995) determined that the New Creek and Corriganville interval formed a very condensed 4^{th}-order sequence, which consisted of only two 5^{th}-order sequences. In the current study, the New Creek-Corriganville interval is still considered to be a 4^{th}-order sequence based on the major facies changes at its boundaries. However, the total number of cycles in each formation indicates that there must be more 5^{th}-order sequences than have been described previously.

In addition to the numerical stacking patterns of the hierarchic model the symmetry of each rank must be considered. The symmetry of a 5^{th}-order is similar in its pattern to that of an individual 6^{th}-order cycle in that each has a generally asymmetric shallowing-upward pattern (Figure 7). However, the precise form and pattern of 5^{th}-order symmetry is modulated by eccentricity which either enhances or dampens the precessional signal. The enhancement effect is expressed in the major facies change at 5^{th}-order boundaries; the dampening effect is seen in the progressively smaller facies changes at precessional cycle boundaries later in the sequence. Hence an ideal 5^{th}-order sequence, which is composed of five precessional cycles, begins with a major facies change to a significantly deeper facies than the facies below. Then, a second enhanced precessional rise produces the deepest facies in the second cycle, after which the pattern of facies episodically shallows upward, each successive precessional cycle containing shallower facies.

In this study, the cyclic framework of the two formations has been divided into lower and upper parts, possibly corresponding to short eccentricity cycles, based on the major facies changes at their basinwide bounding surfaces. Within the New Creek Formation, a possible 5^{th}-order boundary between PACs 3 and 4 (Figures 10, 11, 13 and 17) separates the massively bedded lower half of the formation from more argillaceous and thinly bedded upper half. Given the dramatic facies change at the New Creek-Corriganville contact which indicates a definite 5^{th}-order sequence boundary, the New Creek interval is therefore interpreted as two 5^{th}-order sequences, each consisting of three precessional cycles. The implication is that both of the 5^{th}-orders are incomplete; confirmation of degree of incompleteness awaits correlation with potentially more complete sections in New York State. It has been determined (Sullivan and Anderson, 1986) that the Keyser-New Creek contact is unconformable and that there was a period of exposure and differential erosion of Keyser cycles. This event may represent a long period of time during which there was no deposition, which would result in New Creek cycles being missed by hiatus. However, it is plausible that the cycles missing at the contact in the study section are deposited elsewhere in the deeper parts of the basin.

Another possibility is that, especially since at some localities there are only five cycles detected in the New Creek Formation, the whole of New Creek Formation indeed consists of one 5^{th}-order sequence as described previously. This idea is supported by the fact that in the Lower Paleozoic the duration of a precessional cycle was in between 16 ky and 18 ky (Berger, 1988), which, given six precessional cycles, would give a total of 98 ky for a 5th-order sequence.

The Corriganville Formation follows a pattern to that in the New Creek Formation; in the lower half, the bedding style is more massive as opposed to the thin, more argillaceous and cherty beds of the upper Corriganville Formation. Within the Corriganville Formation, the boundary between the lower and upper Corriganville falls between PACs 3 and 4 (Figures 27 and 28). This boundary is characterized by a medium-grained, massive flat-topped calcarenite at all localities, overlain by a persistent shale with nodular micrite at all localities, and marks the beginning of a thinner-bedded cycles above. The surface between PACs 3 and 4, across which the pattern of allocycles differs, is traceable in its pattern throughout the study area. In the Corriganville Formation, there are three allocycles in the lower portion and six in the upper portion. The symmetry and stacking of the lower 5th-order are incomplete. The upper 5th-order contains six precessional cycles; as discussed above, the precessional cycle duration could have been as short as 16 ky in the Lower Paleozoic (Berger, 1988), making this 5th-order complete.

The symmetry of the 4th-order may be similar to the symmetry of the 5th-order (Anderson and Goodwin, 1992). Hence, the second 5th-order should be the deepest, though in the study section this is not the case. The New Creek Formation as a whole is shallower than the Corriganville Formation; within the Corriganville Formation, the second 5th-order appears deeper than the first 5th-order sequence. Furthermore, the large-scale trend (Keyser-New Creek-Corriganville-Mandata) is transgressive and hence the sequence is deepening as a whole. The cause for this trend is subsidence, which begun to affect the basin in steadily increasing manner. Accelerating subsidence combined with Milankovitch eustasy to produce successively deeper 5th-order packages. The combined dynamics of eustatic sea-level fluctuations and increasing subsidence are the causes for the patterns observed in the New Creek-Corriganville Sequence, and hence may be the cause for missing cycles and atypical stacking patterns.

Partial answers to questions of fourth-order completeness and symmetry may lie in the correlation of the sequence with thicker sections to the north-east and south. The Corriganville Formation thickens markedly southward in Maryland and West Virginia (Dorobek and Read, 1986), which may indicate either that the cycles potentially missing in the studied interval were deposited there, or that the individual cycles are thicker. To the north, at Muncy, PA, where the Corriganville is also much thicker (30 ft; 9.14 m), the interval seems to have a cyclic structure very similar to that in the study interval. Farther north the correlations with the Helderberg sequence in New York State are still uncertain (P.W. Goodwin, 1996, personal communication). Those sections, which are considerably thicker and probably more complete, whatever the precise correlations, will likely provide information on the 4th-order structure of the New Creek-Corriganville interval.

CHAPTER 5
A SMALL-SCALE STRATIGRAPHIC MODEL FOR THE ORIGIN OF CHERT

Introduction

The consistent association of chert with elements of the allocyclic stratigraphic fabric of the New Creek and Corriganville Formations suggests that there is a genetic link between the occurrence of chert and that stratigraphic fabric. In the New Creek Formation, chert occurs typically at cycle boundaries; in the Corriganville Formation, chert occurs additionally in high-stand parts of cycles and at sea-level-fall surfaces. This correspondence of stratigraphic surfaces and parts of cycles with occurrence of chert beds indicates that the primary stratigraphic process responsible for the allostratigraphic fabric, that is high-frequency sea-level fluctuations, is in some manner responsible for the distribution of chert in these formations.

Based on observation and analysis of facies patterns and chert occurrences in the New Creek and Corriganville Formations the following model offers a partial explanation of the stratigraphic control of the formation of chert. This model will indicate a possible source of concentrated silica and a plausible connection between high-frequency sea-level changes and the process of silicification in below-wave-base carbonate facies. In this model the characteristics of silica formation, accumulation, preservation, and dissolution/precipitation are affected by stratigraphic processes.

Accumulation of Silica

PAC boundaries are non-depositional surfaces formed during precessional sea-level rises (Figure 4); these times of non-deposition of carbonate and siliciclastic sediments provide optimal conditions for the accumulation of silica (Figure 38). At these times of highest rate of sea-level rise, when the production of carbonate sediments ceases and siliciclastics are trapped in the fluvial systems, organic silica and silica-rich volcanic ash can accumulate undiluted by other sediments. Sponges grow in abundance in quiet, near-wave-base environments (Zhang and Pratt, 1994), where sponges proliferate on hardground surfaces which result from the rapid rise of sea-level. The other source of organic silica in the Lower Paleozoic was radiolarians; these siliceous organisms are planktonic, and proliferate in the photic zone of water column regardless of the variation in the water depth. The accumulation of radiolarians is preferentially greater during times of non-deposition (hardgrounds), because there is no other significant accumulation of sediments. Low-energy conditions of the below-wave-base environment further enhance the preservation potential of siliceous matter. Geochemically, siliceous matter is protected from dissolution by the accumulation of clay and organic matter, which form an impermeable membrane limiting interaction with sea-water. Another geochemical preservational factor is the total quantity and type of siliceous matter; greater accumulation rates and thus total quantity of silica enhance the likelihood of preservation in the sediments (Hein *et al.*, 1989). This preservation is affected by both the dissolution dynamics of siliceous particles (*e.g.* Williams *et al.*, 1985a); particles with greater surface area are more likely to be dissolved. Likewise, greater quantity of siliceous matter

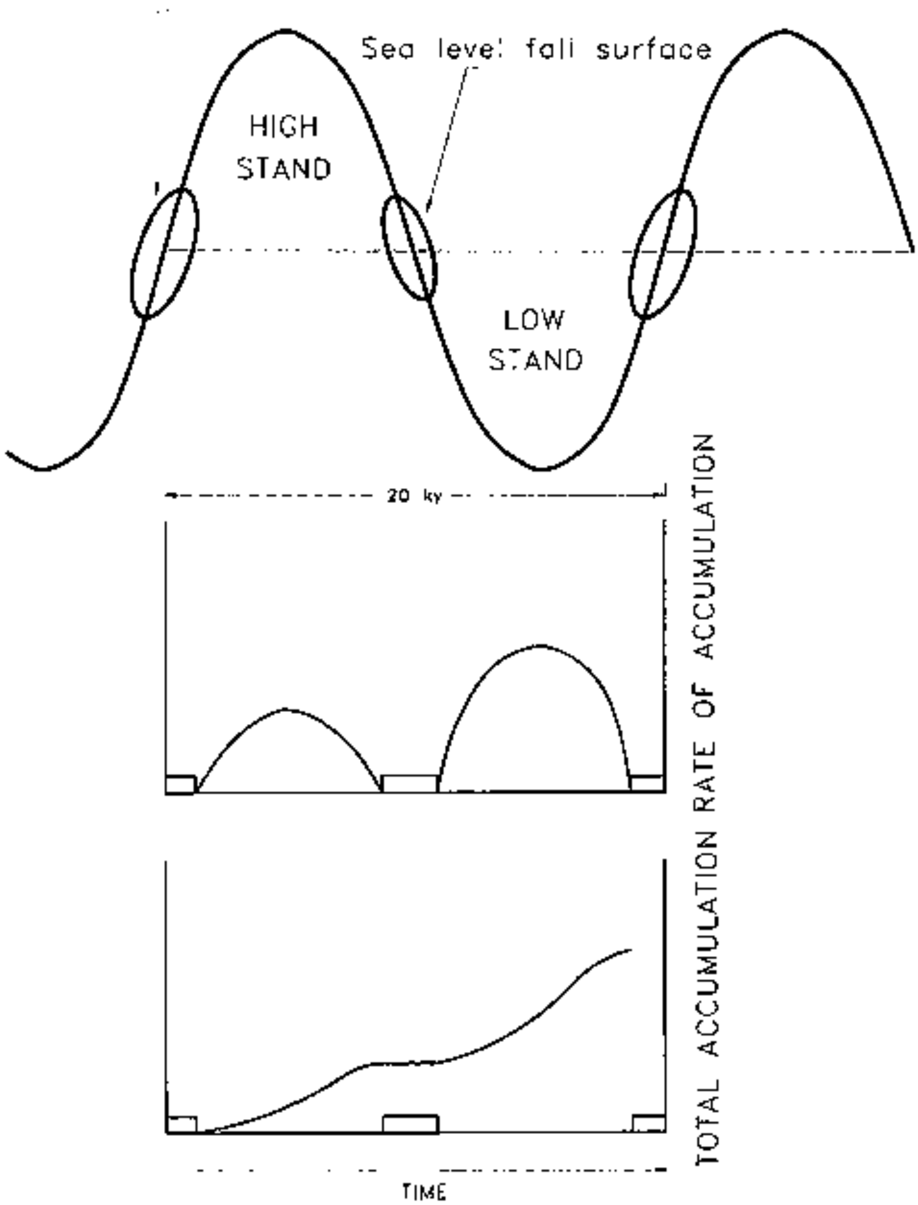

Figure 38. PAC dynamics: Accumulation diagram.

The pattern of sedimentation responds to the precessional eustatic sea-level curve in the making of an ideal PAC. Rate of sediment accumulation is greatest between cycle boundaries (the low rectangles on the x-axis reflecting non-depositional PAC boundaries). Total accumulation reflects the pattern of rate of accumulation by increasing within cycles and remaining constant at cycle boundaries and sea-level-fall surfaces.

will have less overall surface exposed to sea water. Even though PAC boundaries are optimal in regard to silica accumulation, chert is found also at sea-level-fall surfaces and in the high-stand portions of cycles in the Corriganville Formation. Sea-level-fall surfaces result from rapid falls of sea level, which produce surfaces of non-deposition. As at cycle boundaries, times of non-deposition during rapid sea-level falls permit accumulation of organic silica undiluted by carbonate and terrigenous sediments. The high-stand portions of the cycles in the Corriganville Formation are characterized by intermittent deposition, which occurs in deeper and lower energy conditions relative to conditions in the low-stand portions. Under these relatively sediment-starved conditions proportionately more silica can accumulate. In addition, these high-stand portions contain abundant clay and organic matter, which promote silica preservation after the initial accumulation and are important ingredients in silicification.

Silicification

The diagenetic conditions which promote silicification and replacement of carbonate are partially controlled by stratigraphic processes. For example, clay and organic matter, which are associated with cycle boundaries, sea-level-fall surfaces and high-stand portions of Corriganville PACs, are vital participants in the replacement process. After burial, reducing conditions promote the formation of a diagenetic environment conducive to silicification. Reducing conditions can be produced within a zone (*e.g.* sulphate reduction zone) or a point (*e.g.* soft tissues in a brachiopod). The sulphate reduction zone is dependent both on depth and on the presence of diagenetic ingredients such as dissolved sulphate, organic matter, dissolved iron, and lack of oxygen (Berner, 1984). During the hiatus at a cycle boundary, a particular diagenetic zone (*e.g.* sulphate reduction zone) acts longer at a particular horizon within the sediments, thus enhancing diagenesis in the sediments immediately below the non-depositional surface. A longer hiatus in sedimentation at a cycle boundary may result in a greater degree of diagenesis by allowing certain reactions to occur for longer period of time, and ultimately in more complete silicification and replacement of host carbonates. The greater degree of silicification and the accompanying loss of detail observed in Corriganville chert may be the result of longer hiatus at cycle boundaries in the deeper, sediment-starved environments of that formation.

In addition to the difference in the length of hiatus at cycle boundaries, absolute depth may have contributed to the greater degree of silicification in the Corriganville Formation. For example, in the Arkansas Novaculite (Devonian to Mississippian), shallow platform cherts featured well preserved details of sponge spicules, radiolarians and early diagenetic textures, while in the deeper parts of the basin fossils were preserved only as ghosts and early diagenetic features were lost (Jones and Knauth, 1979). In the shallower environment silicification might have been more rapid because of increased hydraulics; in the deeper part of the basin, burial diagenesis was dominant (Jones and Knauth, 1979). Since the silicification was more rapid in the shallower part, early diagenetic features were "preserved" in the chert (Meyers, 1977) whereas in the deeper part diagenesis had commenced further before extensive silicification. In a similar manner, the deeper Corriganville Formation may have experienced greater diagenesis and slower silicification before full chertification.

The cycle boundaries in the New Creek and Corriganville Formations are lined with clay; clay and other impurities, which include cations such as Mg^{2+}, Mn^{2+}, Fe^{2+} and Al^{3+}, promote nucleation and other diagenetic reactions in the process of silicification. Iron is associated with the sulphate reduction zone and pyrite formation; other cations operate as nucleation sites and may lower the required pH for polymerization and nucleation of silica. Permeable facies near cycle boundaries may be conduits for silica in solution; associated clay at cycle boundaries would direct the flow of pore waters horizontal to bedding planes. The preferential association of chert near cycle boundaries indicates that the boundary conditions are a more important variable than absolute porosity and permeability controls; all kinds of lithology, from coarse fossil hash to micrite, have been silicified in the New Creek and Corriganville sequence.

Conclusion

The association of chert with cycle boundaries, sea-level-fall surfaces and high-stand parts of the cycles in the Corriganville Formation is controlled by stratigraphic processes. At cycle boundaries and sea-level-fall surfaces the control is by cessation of carbonate and siliciclastic sediments during rapid sea-level rise, thus allowing siliceous sediments to accumulate without being diluted. The shaley high-sand portion of Corriganville cycles which accumulated in deeper, low-energy environments also contain the prerequisites of chert formation: intermittent deposition in starved conditions;

abundance of clay; and organic matter. Preservation of delicate opaline matter at sratigraphic surfaces is enhanced by its abundance and by the accumulation of clay-rich sediments which prevent dissolution by sea water. The stratigraphic process of high-frequency sea-level change may also play a role in enhancing diagenesis in the sediments immediately below a non-depositional surface, because diagenetic zones remain in a stable position during this time of depositional hiatus. Hence the occurrence of chert is controlled primarily by stratigraphic processes and secondarily by sedimentological and geochemical factors.

CHAPTER 6
CONCLUSIONS

1. The New Creek and Corriganville Formations are entirely divisible into correlative small-scale (1.5 ft/0.46 m) cycles.

2. These correlative, small-scale cycles are interpreted to be 6^{th}-order, precessional cycles (PACs), which are bundled into eccentricity-modulated 5^{th}-order sequences.

3. The study interval as a whole is a 4^{th}-order sequence consisting of three or four incomplete 5^{th}-order sequences.

4. The occurrence of chert beds and nodules is concentrated at 6^{th}-order cycle boundaries within the study interval. In the Corriganville Formation, chert occurs additionally at sea-level-fall surfaces and in the high-stand portions of the cycles.

5. The persistent correspondence of chert occurrence with the allostratigraphic framework suggests that the same process responsible for the stratigraphic fabric, namely high-frequency sea-level changes, also controlled chert occurrence by:

   a. Permitting undiluted accumulation of silica (*i.e.* sponge spicules, radiolarians, volcanic ash) on non-depositional surfaces (*i.e.* cycle boundaries and sea-level-fall surfaces) and in sediment-starved sedimentary environments (*i.e.* high-stand portions of Corriganville PACs).

   b. Enhancing diagenesis in the sulphate reduction zone during times of hiatus at cycle boundaries and sea-level-fall surfaces when the sediment-water interface remained stable.

6. Variations in chert morphology, and degree and pattern of silicification, indicate that silicification was controlled secondarily by textural and compositional inhomogeneities in the sediments, that provided conduits for fluids transporting dissolved silica from primary areas of concentration.

7. The greater degree of silicification and loss of detail in the Corriganville cherts are attributed to longer time of non-deposition at cycle boundaries and thus longer reaction time in the sulphate reduction zone, and to a generally more favorable environment containing more of the geochemical ingredients of silicification.

8. Results of this study suggest that future studies of the origin of chert need to consider the role of stratigraphic processes in the positioning of chert beds and nodules.

REFERENCES CITED

Anderson, E.J. and Goodwin, P.W., 1990, The significance of meter-scale allocycles in the quest for a fundamental stratigraphic unit: Journal of the Geological Society, v. 147, p. 507-518.

Anderson, E.J., and Goodwin, P.W., 1992, What distinguishes PACs from parasequences?, Abstracts with Programs, Northeastern Geological Society of America, v.24, No. 3, p. 3.

Anderson, E.J., Goodwin, P.W., and Goodman, P.T., 1986, Reconstruction of patterns of differential subsidence using an episodic stratigraphic model, *in* Allen, Phillips A. and Homewood, Peter, eds., Foreland Basins, IAS Special Publications No. 8: Williams Clowes Limited, Beccles and London, p. 437-443.

Anderson, E.J., Goodwin, P.W., and Sobieski, T.H., 1984, Episodic accumulation and the origin of formation boundaries in the Helderberg Group of New York State: Geology, v. 12, p. 120-123.

Aplin, A.C., and Warren, E.A., 1994, Oxygen isotopic indications of the mechanisms of silica transport and quartz cementation in deeply buried sandstones: Geology, v. 22, p. 847-850.

Baltuck, M., 1986, Authigenic silica in Tertiary and Upper Cretaceous sediments of the East Mariana Basin, site 585: Initial Reports the Deep Sea Drilling Project, *in* Moberly, R. and others, Initial Reports Deep Sea Drilling Project, v. 89: Washington (U.S. Government Printing office), p. 389-398.

Bennett, P. and Siegel, D., 1987, Increased solubility of quartz in water due to complexing by organic compounds: Nature, v. 326, p. 684-686.

Berger, A., 1988, Milankovitch theory and climate: Review of Geophysics, v. 26, p. 624-657.

Berner, R., 1984, Sedimentary pyrite: An update: Geochimica et Cosmochimica Acta, v. 48, No. 4, p. 605-615.

de Boer, P.L., and Smith, D.G., 1994, Orbital forcing and cyclic sequence, *in* de Boer, P.L. and Smith, D.G., eds., Special Publications of International Association of Sedimentologists, v. 19: Blackwell Scientific Publications/the Alden Press, Oxford, Great Britain, p. 1-14.

Bohrmann, G., Abelman, A., Gersonade, R., Hubberten, H., and Kuhn, G., 1994, Pure siliceous ooze, a diagenetic environment for early chert formation: Geology, v. 22, p. 207-210.

Brett. C. and Ver Straeten, C., 1994, Stratigraphy and facies relationships of the Eiffelian Onondaga Limestone (Middle Devonian) in Western and West Central New York State, *in* Brett, C. and Scatterday, J., eds, Field Trip Guidebook, 66th Annual Meeting, New York State Geological Association, p. 221-324.

Bromley, R.G. and Ekdale, A.A., 1986, Flint and chalk in the European Chalk; *in* de G. Sieveking, G. and Hart, M.B., The Scientific Study of Flint and Chert: Cambridge University Press, Cambridge, Great Britain, p. 71-82.

Bustillo, M.A. and Ruiz-Ortiz, P.A., 1987, Chert occurrences in carbonate turbidites: examples from the Upper Jurassic of the Betic Mountains (southern Spain): Sedimentology, v. 34, p. 611-621.

Chadwick, W., 1994, Correlation of Milankovitch-cyclicity in the peritidal carbonates of the Tonoloway Formation, Central Pennsylvania and Western Maryland, [Master's Thesis]: Temple University.

Chanda, S.K., Bhattacharyya, A., and Sarkar, S., 1976, Early diagenetic chert nodules in Bhander Limestone, Maihar, Satna District, Madhya Baresh, India: Journal of Geology, v. 84, p. 213-224.

Clayton, C.J., 1986, The diagenetic environment of flint formation in Upper Cretaceous Chalks, *in* de G. Sieveking, G. and Hart, M.B., The Scientific Study of Flint and Chert: Cambridge University Press, Cambridge, Great Britain, p. 43-54.

Connor, J.M., 1983, PAC Analysis of the Dicelosia Epibole in the Lower Devonian Kalkberg Formation, Eastern NY State: [Master's Thesis], Temple University, 88 p.

Dorobek, S.L. and Read, J.F., 1986, Sedimentology and basin evolution of the Siluro-Devonian Helderberg Group, Central Appalachians: Journal of Sedimentary Petrology, v. 56, p. 601-613.

Elorza, J. and Garcia-Garmilla F., 1993, Chert appearace in the Cueva-Bedon carbonate platform (Upper Cretaceous, northern Spain): Geological Magazine, v. 130, p. 805-816.

Eskel, T.M., and Goodwin, P.W., 1994, Allostratigraphic control of the occurrence of chert: Lower Devonian, Central Appalachians: Abstracts with Programs, Northeastern Geological Society of America, v. 26, No 3, p 16.

Felder, P.J., 1986, Rhythms, flint and mesofossils in the Cretaceous (Maastrichtian) of Limburg, the Netherlands, *in* de G. Sieveking, G. and Hart, M.B., The Scientific Study of Flint and Chert: Cambridge University Press, Cambridge, Great Britain, p. 83-88.

Frondel, C., 1978, Characters of quartz fibers: American Mineralogist, v. 63, p.17-27.

Frondel, C., 1985, Systematic compositional zoning in the quartz fiber agates: American Mineralogist, v. 70, p. 975-979.

Gao, G., and Land, L.S., 1991, Nodular chert from the Arbuckle Group, Slick Hills, SW Oklahoma: a combined field, petrographic and isotopic study: Sedimentology, v. 38, p. 857-870.

Geeslin, J.H., and Chafetz, H.S., 1982, Ordovician Aleman ribbon cherts: an example of silicification prior to carbonate lithification: Journal of Sedimentary Petrology, v. 52, No. 4, p. 1283-1293.

Goodman, W.M. and Brett, C.E., 1994, Roles of eustasy and tectonics in development of Silurian stratigraphic architecture of the Appalachian foreland basin: Tectonic and Eustatic Controls on Sedimentary Cycles, SEPM Concepts in Sedimentology and Paleontology No. 4: SEPM, Tulsa, Oklahoma, p. 147-169 .

Goodwin, P.W., and Anderson, E.J., 1985, Punctuated Aggaradational Cycles: A general hypothesis of episodic stratigraphic accumulation: Journal of Geology, v. 93, p. 515-533.

Goodwin, P.W. and Anderson, E.J., 1988, Episodic development of Helderbergian paleogeography, New York State, Appalachian Basin, *in* McMillan N.J., Embry, A.F. and Glass D.J., eds., Devonian of the world: Proceedings of the second international symposium on the Devonian system: Canadian Society of Petroleum Geologists, v. 14, p. 553-567.

Goodwin, P.W., Anderson, E.J., Goodman, W.M., and Saraka, L.J., 1986, Punctuated Aggradational Cycles: implications for stratigraphic analysis, *in* Arthur, Michael A. and Garrison, R.E., eds., Milankovitch cycles through time, Palaeoceanography, v. 1, p. 417-429.

Goodwin, P.W., Anderson, E.J., Saraka, L.J., and Goodman, W.M., 1985, Correlation of punctuated aggradational cycles, Helderberg Group, between Schoharie and Thacher Park, New York State Geological Association, 57th Annual Meeting, Field Trip Guidebook, p. 68-81.

Graber, K.K., and Chafetz, H.S., 1990, Petrography and origin of bedded barite and hosphate in the Devonian Slaven chert of Central Nevada: Journal of Sedimentary Petrology, v. 60, p. 897-911.

Heaney, P.J., Veblen, D.R., and Post, J.E., 1994, Structural disparities between chalcedony and macrocrystalline quartz: American Mineralogist, v. 79, p.452-460.

Heling, D., and Giskow, R., 1994, Tranport of matter in sediments: A discussion, *in* Heling, G., Rothe, P. Forstner, U. and Stoffers, P., eds, Sediments and Environmental Geochemistry: Springer-Verlag, Berlin Heidelberg, p. 339- 350.

Hein, J.R., Hseuh-Wen Y., and Barron, J.A., 1989, Eocene diatom chert from Adak Island, Alaska: Journal of Sedimentary Petrology, v. 60, p. 250-257.

Hendry, J.P., 1993, Calcite sedimentation during bacterial manganese, iron and sulfate reduction in Jurassic shallow marine carbonates: Sedimentology, v. 40, p. 87-106.

Hesse, R., 1987, Selective reversible carbonate-silica replacements in Lower Cretaceous carbonate-bearing turbidites of the Eastern Alps: Sedimentology, v. 34, p. 1055-1077.

Hesse, R., 1988, Diagenesis; Origin of chert: Diagenesis of biogenic siliceous sediments: Geoscience Canada, v. 15, p. 171-192.

Hesse, R., 1989, Silica diagenesis: Origin of inorganic and replacement cherts: Earth Science Reviews, v. 26, p. 253-284.

Honigstein, A., Lipson-Benita, S., Conway, B., Flexer, A., and Rosenfeld, A., 1989, Mid-Turonian anoxic event in Israel- a multidisciplinary approach: Palaeogeography, Palaeoclimatology, Palaeoecology, v. 61, p. 103-112.

Jones, D.L., and Knauth L.P., 1979, Oxygen isotopic and petrographic evidence relevant to the origin of the Arkansas Novaculite: Journal of Sedimentary Petrology, v. 49, No. 2, p. 581-598.

Kolodny, Y., 1986, The origin of cherts as members of high productivity sequences: isotopic evidence, *in* de G. Sieveking, G. and Hart, M.B., The Scientific Study of Flint and Chert: Cambridge University Press, Cambridge, Great Britain, p. 55-62.

Laporte, L.F., 1969, Recognition of a transgressive carbonate sequence within an epeiric sea: Helderberg Group (Lower Devonian) of New York State, *in* Friedman, G.M., ed., Depositional Environments of Carbonate Rocks: SEPM Special Publications, v. 14, p. 98-119.

Lawrence, M., 1994, Conceptual model for early diagenetic chert and dolomite, Amuri Limestone Group, north-eastern South Island, New Zealand: Sedimentology, v. 41, p. 479-498.

Loope, D.B., and Watkins, D.K., 1989, Pennsylvanian fossils replaced by red chert: early oxidation of pyrite precursors: Journal of Sedimentary Petrology, v. 59, No. 3, p. 375-386.

Maliva, R.G., 1987, Quartz geodes: Early diagenetic silicified anhydrite nodules related to dolomitization: Journal of Sedimentary Petrology, v. 57, No. 6, p. 1054-1059.

Maliva, R.G., and Siever, R., 1988, Mechanisms and controls of silicification of fossils in limestones: Journal of Geology, v. 96, p. 387-398.

Maliva, R.G., and Siever, R., 1989, Chertification histories of some Late Mesozoic and Middle Palaeozoic platform carbonates: Sedimentology, v. 36, p. 907-926

Matheney, R.K., and Knauth, L.P., 1993, New isotopic temperature estimates for early silica diagenesis in bedded cherts: Geology, v. 21, p. 519-522.

Meyers, W.J., 1977, Chertification in the Mississippian Lake Valley Formation, Sacramento Mountains, New Mexico: Sedimentology, v. 24, p. 75-105.

Misik, M., 1993, Carbonate rhombohedra in nodular cherts: Mesozoic of the West Carpathians: Journal of Sedimentary Petrology, v. 63, No 2, p.275-281.

Mortimore, R.N., 1986, Controls on upper Cretaceous sedimentation in the South Downs, with particular reference to flint distribution, *in* de G. Sieveking, G. and Hart, M.B., The Scientific Study of Flint and Chert: Cambridge University Press, Cambridge, Great Britain, p. 21-42.

Mortimore, R.N. and Wood, C.J., 1986, The distribution of flint in the English Chalk, with particular reference to the "Brandon Flint Series" and the high Turonian flint maximum, *in* de G. Sieveking, G. and Hart, M.B., The Scientific Study of Flint and Chert: Cambridge University Press, Cambridge, Great Britain, p.7-20.

Namy, J.N., 1974, Early diagenetic chert in the Marble Falls Group (Pennsylvanian) of Central Texas: Journal of Sedimentary Petrology, v. 44, p. 1262-1268.

Noble, J.P.A. and van Stempvoort, D.R., 1989, Early burial quartz authigenesis in Silurian platform carbonates, New Brunswick, Canada: Journal of Sedimentary Petrology, v. 59, p. 67-76.

Oliver, W.A, 1956, Stratigraphy of the Onondaga Formation in eastern New York: Bulletin of the Geological Society of America, v. 67, p. 1441-1474.

Orzechowski, C., 1995, Recognition of Milankovitch orbital forcing patterns in shelf facies of the Lower Devonian New Creek and Corriganville Formations of Central Pennsylvania: [Master's Thesis], Temple University, 63 p.

Raiswell, R., 1987, Non-steady state microbiological diagenesis and the origin of concretions and nodular limestones, *in* Marshall J.D., ed., Diagenesis of Sedimentary Sequences, Geological Society Special Publication No. 36: Blackwell Scientific Publications, Oxford, Boston, p. 41-54.

Read, J.F., Grotzinger, J.P., Bova, J.A., and Koerschner, W.F., 1986, Models for generation of carbonate cycles: Geology, v. 14, p. 107-110.

Rice, S.B., Freund, H., Huang, W.-L., Clouse, J.A., and Isaacs, C.M., 1995, Application of Fourier transform infrared spectroscopy to silica diagenesis: the opal-A to opal-CT transformation: Journal of Sedimentary Research, v. A65, p. 639-647.

Rickard, L.V., 1962, Late Cayugan (Upper Silurian) and Helderbergian (Lower Devonian) stratigraphy of New York, New York State Museum and Science Series Bulletin, Albany, New York, v. 386, 157 p.

Robertson, A.H.F., 1977, The origin and diagenesis of cherts from Cyprus: Sedimentology, v. 24, p. 11-30.

Schulz, H.D., Dahmke, A., Schinzel, U., Wallman, K., and Zabel, M., 1994, Early diagenetic processes, fluxes, and reaction rates in sediments of the South Atlantic: Geochimica et Cosmochimica Acta, v. 58, No. 9, p. 2041-2060.

Schwarzacher, W., 1993, Cyclostratigraphy and the Milankovitch theory, (Developments in Sedimentology, v. 52), Amsterdam, Netherlands: Elsevier, 207 p.

Siever, R., 1962, Silica solubility, 0°-100° C., and the diagenesis of siliceous sediments: The Journal of Geology, v. 70, p. 127-150.

Strasser, A., 1994, Milankovitch cyclicity and high-resolution sequence stratigraphy in lagoonal-peritidal carbonates (Upper Tithonian-Lower Berriasian, French Jura Mountains): Special Publications of the International Association of Sedimentology, v. 19, p. 285-301.

Walther, J.V. and Helgeson, H.C., 1977, Calculation of the thermodynamic properties of aqueous silica and the solubility of quartz and its polymorphs at high temperatures and pressures: American Journal of Science, v. 277, No. 10, p. 1315-1351.

Van Wagoner, J. C., Posamentier, H.W., Mitchum, R.M., Vail, P.R., Sarg, J.F., Loutit, T.S., and Hardenbol, J., 1988, An overview of the fundamentals of sequence stratigraphy and key definitions, *in* Wilgus, Cheryl K. *et al.,* Seal-level changes: an integrated approach, SEPM Special Publication No. 42: Tulsa, Oklahoma, Society of Economic Paleontologists and Mineralogists, p. 39-45.

Ver Straeten, C., and Brett, C., 1995, Lower and Middle Devonian Foreland Basin in the Catskill Front: Stratigraphic synthesis, sequence stratigraphy and the Acadian Orogeny, *in* Fieldtrip Guide for the 67th Annual Meeting of the New York State Geological Association, New York State Geological Association, NY, p. 313-356.

Williams, L.A., Parks, G.A., and Crerar, D.A., 1985a, Silica diagenesis; I Solubility controls: Journal of Sedimentary Petrology, v. 55, No. 3, p. 301-311.

Williams, L.A., and Crerar, D.A., 1985b, Silica diagenesis; II General mechanisms: Journal of Sedimentary Petrology, v. 55, No. 3, p. 312-321.

Zhang, X., and Pratt, B.R., 1994, New and extraordinary Early Cambrian sponge spicule assemblage from China: Geology, v. 22, p. 43-46.

APPENDIX A
DESCRIPTION OF FIELD LOCALITIES

1. Cessna

Lat. 40°06'45"N, long. 78°31'30"W. Bedford 7.5 min. Quadrangle, PA. Roadcut on U.S. Route 220, on southbound lane, 4.5 miles (7.2 km) north of Pennsylvania Turnpike Overpass.

2. St. Clairsville

Lat. 40°08'25"N, long. 78°30'15"W. Alum Bank 7.5 min. Quadrangle, PA. Roadcut on U.S. Route 220, southbound lane, on exit ramp to St. Clairsville, PA, 9.5 miles (15.3 km) north of Pennsylvania Turnpike overpass.

3. Hollidaysburg

Lat. 40°26'00"N, long. 78°22'28"W. Frankstown 7.5 min. Quadrangle, PA. Roadcut on U.S. Route 22, 1.2 miles (2 km) east of intersection of U.S. Route 22 and State Route 36.

4. Canoe Creek Quarry

Lat. 40°29'16"N, long. 78°17'44"W. Frankstown 7.5 min. Quadrangle, PA. Abandoned quarry on Malvern Road, 3.4 miles (5.4 km) on Malvern Road from Route 22, 6.8 miles (11 km) from intersection of U.S. Route 22 and U.S. Route 36.

4. Altoona Bypass/Eldorado Quarry

Lat. 40°27'35"N, long. 78°25'20"W. Hollidaysburg 7.5 min. Quadrangle, PA. Abandoned quarry on U.S. Route 220, northbound lane, 2.5 miles (4 km) north from intersection of old State Route 22 and Pennsylvania Turnpike.

5. Allegheny Furnace

Lat. 40°29'40"N, long. 78°24'28"W. Hollidaysburg 7.5 min. Quadrangle, PA. Abandoned quarry behind the parking lot of Christian Science and Baptist Church in Altoona, on U.S. Route 36, 1.3 miles (2.1 km) north of State Route 36 and Pleasant Valley Boulevard.

6. Tyrone

Lat. 40°40'40"N, long. 78°14'36"W. Tyrone 7.5 min. Quadrangle, PA. An abandoned quarry behind American Legion Post on State Route 453 in Tyrone, 1 mile (1.6 km) north-west of U.S. Route 220 overpass.

7. Limestoneville

Lat. 41°01'50"N, long. 76°44'09"W. Washingtonville 7.5 min. Quadrangle, PA. Active quarry, Lycoming Silica Sand Quarry, on State Route 254, 6 miles (9.6 km) west of Milton.

8. Grovania

Lat. 40°58'25"N, long. 76°31'31"W. Danville 7.5 min. Quadrangle, PA. Active quarry, Lycoming Silica Sand Quarry, on U.S. Route 11, 4.5 miles (7.2 km) west of Danville.

APPENDIX B
COMPARATIVE STUDY ON CHERT LITERATURE

Author	Baltuck, 1989	Clayton, 1986	Elorza and Garcia-Camilla, 1993
Age	Tertiary- Upper Cretaceous	Cretaceous	Cretaceous
Composition	chert, limestone, claystone; chert: almost complete silica	Chalk; flint bands	microquartz, chalcedony, megaquartz
Relict Features	silicified limestone:silica cement and carbonate	burrows; flint occurs in horizons	grainstone, packstone, Thalassinoides burrows
Paleoenvironment	depth 6100 m, near equator	shallow shelf	carbonate platform
Stratigraphy	East Mariana Basin; chert, limestone and claystone sequences, no correlation	a section in British Cretacous chalk	sequence stratigraphy: above type 1 sequence boundary
Source of Silica	radiolarians	biogenic	sponge spicules, radiolarians
Process	diagenesis related to composition: MgOH2, porosity, permeability enhances, hence clay impedes	diagenesis related to diagenetic reactions acting at a particular horizon during sedimentation pause	opal-CT lepispheres: maturation process, oxygen isotopes: marine

Author	Gao and Land, 1991	Geeslin and Chafetz, 1982	Graber and Chafetz, 1990
Age	Early Ordovician	Ordovician	Devonian
Composition	microquartz, fibrous and microflamboyant;cement chalcedony and megaquartz	chert interlayered with dolomite; microquartz, chalcedony, megaquartz	barite: nodules, crypto- and fine crystalline; chert: chalcedony and megaquartz
Relict Features	grainstone, burrow filling, algal structures, evaporite nodules: porosity, permeability, organic matter; evaporite with early dolomite	relict grainstone, local texture; most chert preferentially algal mats	primary chert: none; organic matter rich microfacies has phosphate in interbedded barite and silica
Paleoenvironment	intertidal -subtidal, shallow platform	intertidal to subtidal	barite in silica: seafloor discharge of subsurf. fluids; redox conditions; oxygen starved, outer shelf to slope
Stratigraphy	nodules in a horizon, evaporitic throughout; no cyclic interpretation	chert nodules in horizons; ribboned chert and dolomite 12-20 m	50 m column of barite and chert
Source of Silica	sponge spicules and sea-water: sponge spicules in limestone	sponge spicules: axial canals, triaxon shape	sponge spicules and quartz silt
Process	lepisphere structure preserved; nucleation control by porosity, permeability, organic matter	silicification before dolomitization; seasonal variation produced cyclic structure; phreatic mixing zone	fatty acids: sulfate reducing bacteria?

Author	Hart and Swiecicki, 1986	Knauth and Lowe, 1978	Kovasz and Tardi-Filazs, 1994
Age	Cenomanian to Maastrichtian	Archean, 3.4 billion years	Jurassic- Cretaceous
Composition	micritic limestone, carbonate debris, planktonic algae	granular microcr. chert; chalcedony, megaqtz; dolomite rhombs in chert matrix; silicified evaporites	radiolarites and calpionellids in white limestone; chert abundance not correlated with rad. occurrence
Relict Features	fine fraction: coccoliths	volcaniclastic detritus, limestone	white cherty limestone
Paleoenvironment	benthonic: Foram. in a soft carbonate ooze with bivalves, bryozoa		deep water pelagic, around aragonite CCD and lysocline
Stratigraphy	abrupt changes in fauna; limestone/marl and chalk/flint rhythm	14 000 m of interbedded lavas, pyroclastic units, sedimentary rocks with chert	thin limestone beds, chert nodules, inverse relation with rad. and calp. abundance
Source of Silica	? not a chert paper	primary: ocean water	radiolarians
Process	proportion of different planktonic association with global sea-level change	early sil.: synsedimentary brecciation	diagenetic: silica mobilized, rad. tests filled with calcite; upwelling induced production of biogenic silica

Author	Lawrence, 1994	Maliva and Siever, 1988	Maliva and Siever, 1989
Age	Cretaceous-Eocene	Mississ., Dev., Mesoz., Upper Cret.	Late Mesozoic- middle Mesozoic
Composition	chert, dolomite, limestone; organic matter, rhombs, pyrite	mudstone to grainstone; all qtz types, linked to microstr. and pore water silica content	lenght-fast chalcedony, blocky megaquartz, mostly microcrystalline quarzt
Relict Features	trace element	fine detail preserved in fossils	ghosts of pre-chertification carbonate
Paleoenvironment	bathyal to shallow shelf	cratonic platform; shallow water; platform; deeper water pelagic	subtidal marine wackestone and mudstone; around fair-weather wave-base; quiet water, below tide; chert, at 30 100 m
Stratigraphy	measured sections composed of 6 diagenetic zones with varying compositions	grouping according to formation	distribution of nodular chert is restricted; five carbonate sequences described; by formation
Source of Silica	sponge spicules, radiolarians, ocean water?	biogenic	sponge spicules
Process	early diagenetic with pyrite and dolomite, localized oxidation in reduced environment	force of crystallization: pressure induced dissolution	in unsilicified sediments; burial to pressure solution

Author	Meyers, 1977	Misik, 1992	Murchey and Jones, 1992
Age	Mississippian	Mesozoic	Mid-Permian
Composition	mudsupported to grainstone; chalcedony, megaquartz	carbonate rhombohedra in nodular chert,biomicrite	
Relict Features	grains and lime mud, pore filling; preference to mud supported	lepisphere observed in rhombohedra, globular ghosts indicative of radiolaria	associated with phosphorites: upwelling?
Paleoenvironment	skeletal mud- and grainstone, crinoidal and fenestrate bryozoan wackestone and packstone	1. shallow water; 2. pelagic	high productivity zones; drowned shelf to seamount
Stratigraphy	17 measured sections: 70 m on av., some biohermal punctuation	Lower- middle Jurassic crinoidal biosparite; Tithonian biomicrite	
Source of Silica	sponge spicules, intraformational	1. spicules; 2. radiolarians	sponge spicules, radiolarians
Process	mud-supported chertification: intraformational silica source	fluctuating conditions during silicification	

Author	Namy, 1974	Noble and Stempvoort, 1989	Robertson, 1977
Age	Pennsylvanian	Silurian	Campanian-U. Eocene
Composition	Chalcedony, microcrystalline quartz	qzt cement: megaqtz, chalcedony; replacive: microqzt, spherulitic qzt; calcite cement; pyrite, gypsum, dolomite	granular to vitreous chert: cristobalite and qzt
Relict Features	oolite allochems	chalcedony: pores; megaqzt: intraskeletal cavities, fractures, intergranular pores	1. calciturbites, base silic.; 2. condensed chalk with irregular nodular chert bodies
Paleoenvironment	early Pennsylvanian subaerial exposure	near-shore sandst, shale, bioclastic grainst, packst, lime mudst; off-shore siltst., carbonate wackest	ocean floor
Stratigraphy	related to subaerial early Penn. unconformity, sil. decreases from the unconformity; 50 sections measured	two shallowing up cycles; 8 measured localites, scale 5m; qzt in relation to biofacies and environment of deposition	
Source of Silica	sponge spicules		radiolarians
Process	early diagenesis reworked sil. allochems; organic matter contributed to precipitation	bacterial sulfate reduction with oxidation of organic matter, leads to local gradients; shallow sil.	

APPENDIX C
DETAILED CHERT DESCRIPTION

ALLEGHENY FURNACE					
Sample number	AF3	AF2	AF1		
Color	light brown; grey	light brown, blueish white	light grey		
Relict rock type	sparse biomicrite;chertified	sparse biomicrite; chertified	micrite		
Structures					
lamination	1	1	0		
cross bedding	0	0	0		
graded	0	0	0		
bioturbation	1	1	1		
wavy lamination	0	0	0		
convoluted bedding	0	0	0		
Fossils					
detail preserved	1	0	0		
ghosts	1	1	0		
replaced	1	0	1		
sponge spicules	0	0	0		
poor preservation	0	1	0		
Carbonate					
rhombs	0	0	0		
grains	0	1	0		
Hematite	1	0	0		
Pyrite					
crystallites	0	0	0		
disseminated	0	1	0		
ghosts	0	0	0		
massive	0	0	0		
Organic Matter	1	1	0		
Silica					
opaque	0	0	0		
clear	0	0	0		
grains	0	0	0		
Stylolites	0	0	0		

ALTOONA BYPASS					
Sample number	AB10	AB9	AB8	AB7	AB6
Stratigraphic position					
Color	blueish buff	light blue	white	light blue - buff brown	buff brown
Relict rock type	micrite; micrite, chertified	chert; micrite	chert	micrite, chertified; micrite	micrite
Structure					
lamination	1	1	0	1	0
cross bedding	0	0	0	0	0
graded	0	0	0	0	0
bioturbation	1	0	0	0	1
wavy lamination	0	0	0	0	0
convoluted bedding	0	0	0	1	0
Fossils					
detail preserved	0	0	0	0	0
ghosts	0	0	0	0	0
replaced	1	1	1	1	1
sponge spicules	0	1	0	1	1
poor preservation	1	1	1	1	0
Carbonate					
rhombs	1	1	0	1	1
grains	1	1	0	1	1
Hematite	1	1	1	1	0
Pyrite					
crystallites	0	0	0	0	0
disseminated	1	0	0	0	0
ghosts	0	0	0	0	0
massive	0	1	0	0	0
Organic Matter	1	1	0	1	0
Silica					
opaque	1	1	1	0	1
clear	1	0	0	0	0
grains	0	0	0	0	0
Stylolites	0	0	0	0	0

ALTOONA BYPASS.					
Sample number	AB5	AB4	AB3	AB2	AB1
Color	medium grey brown	light grey/ brown	medium grey buff	medium grey buff	medium grey buff
Relict rock type	biomicrite, chertified	micrite	biomicrite	biomicrite, chertified	sparse biomicrite
Structure					
lamination	0	0	0	0	0
cross bedding	0	0	0	0	0
graded	0	0	0	0	0
bioturbation	0	0	1	1	0
wavy lamination	0	1	0	0	0
convoluted bedding	0	0	1	1	0
Fossils					
detail preserved	0	0	1	1	0
ghosts	1	0	1	1	1
replaced	1	0	1	1	1
sponge spicules	0	0	1	1	0
poor preservation	1	0	0	0	1
Carbonate					0
rhombs	0	0	1	0	0
grains	1	1	0	0	0
Hematite	0	0	1	1	0
Pyrite					
crystallites	0	0	0	0	0
disseminated	0	0	0	0	0
ghosts	0	0	1	1	1
massive	0	0	0	0	0
Organic Matter	0	0	?	0	0
Silica					
opaque	0	0	1	1	0
clear	0	0	0	0	0
grains					
Stylolites	0	1	0	1	1

HOLLIDAYSBURG					
Sample number	H13	H12	H11	H10	H9
Color	dark grey	brown grey; blueish white	dark grey; blueish white	dark to medium grey	dark grey
Relict rock type	sparse micrite, incipient silicificatio n	muddy micrite; chert	chert	biomicrite, chertified; micrite	micrite
Structure					
lamination	0	1?	1	0	0
cross bedding	0	0	0	0	0
graded	0	0	0	0	0
bioturbation	0	1	0	0	0
wavy lamination	1	0	0	0	0
convoluted bedding	0	1	1	1	1
Fossils					
detail preserved	0	0	0	0	0
ghosts	0	1	1	1	0
replaced	0	0	1	0	0
sponge spicules	0	1	1	1	0
poor preservation	1	0	0	0	0
Carbonate					
rhombs	0	1	0	1	0
grains	0	0	0	0	0
Hematite	0	0	0	0	0
Pyrite					
crystallites	0	0	0	0	0
disseminated	0	0	0	1	0
ghosts	0	0	0	0	0
massive	1	1	0	0	0
Organic Matter	0	1	0	1	1
Silica					
opaque	0	0	1	1	1
clear	0	0	0	0	0
grains	0	0	0	0	0
Stylolites	0	0	0	0	0

HOLLIDAYSBURG					
Sample number	H8	H7	H6	H5	H4
Color	light grey/ buff	dark medium grey	medium grey	medium grey	medium grey
Relict rock type	micrite	micrite, chertified	micrite	packed biomicrite, chertified	micrite
Structure					
lamination	1	1	1	0	0
cross bedding	0	0	0	0	0
graded	0	0	0	0	0
bioturbation	0	0	1	1	0
wavy lamination	0	0	0	0	0
convoluted bedding	0	0	0	0	0
Fossils					
detail preserved	0	0	0	1	1
ghosts	0	0	0	0	0
replaced	0	1	0	1	0
sponge spicules	0	0	0	0	0
poor preservation	0	0	0		0
Carbonate					
rhombs	0	0	0	0	0
grains	0	0	0	0	0
Hematite	0	0	0	0	0
Pyrite					
crystallites	0	0	0	0	0
disseminated	0	0	0	0	1
ghosts	0	0	0	1	0
massive	0	0	0	0	0
Organic Matter	0	0	0	1	1
Silica					
opaque	0	1	0	0	1
clear	0	0	0	0	0
grains	0	0	0	0	0
Stylolites	0	0	0	0	1

HOLLIDAYSBURG			
Sample number	H3	H2	H1
Color	light greenish grey	medium grey	light greenish grey
Relict rock type	micrite; chertified	micrite	micrite, chertified
Structure			
lamination	0	0	0
cross bedding	0	0	0
graded	0	0	0
bioturbation	0	0	0
wavy lamination	0	0	0
convoluted bedding	0	0	0
Fossils			
detail preserved	0	0	0
ghosts	0	0	0
replaced	0	0	0
sponge spicules	0	0	0
poor preservation	0	0	0
Carbonate			
rhombs	0	0	0
grains	0	0	0
Hematite	0	0	0
Pyrite			
crystallites	1	0	1
disseminated	0	0	0
ghosts	0	0	0
massive	0	0	0
Organic Matter	1	0	1
Silica			
opaque	1	0	1
clear	0	0	0
grains	0	0	0
Stylolites	0	0	0

LIMESTONEVILLE						
Sample number	L6	L5	L4	L3	L2	L1
Color	dark grey	medium grey	light grey	medium grey; dark grey	medium grey	nearly black
Relict rock type	biomicrite, chertified	sparse micrite, chertified	micrite	micrite; micrite, chertified	micrite	sparse biomicrite, chertified
Structure						
lamination	0	0		0	0	0
cross bedding	0	0	0	0	0	0
graded	0	0	0	1	0	1
bioturbation	0	1	0	0	0	0
wavy lamination	0	0	0	0	0	0
convoluted bing	0	0	0	0	0	0
Fossils						
detail preserv.	1	0	1	1	0	1
ghosts	1	1	0	1	0	0
replaced	0	1	0	1	0	0
sponge spicules	0	1	0	1	0	0
poor preservation	0	0	0	0	0	0
Carbonate						
rhombs	1	0	1	1	0	1
grains	0	0	0	0	0	0
Hematite	0	0	0	0	0	0
Pyrite						
crystallites	1	0	0	0	0	0
disseminated	0	0	0	0	0	0
ghosts	1	1	0	0	0	0
massive	0	0	0	1	0	0
Organic Matter	0	0	0	1	0	0
Silica						
opaque	0	0	0	0	0	0
clear	0	0	0	0	0	0
grains	0	0	0	0	0	0
Stylolites	0	0	1	0	1	0

ST. CLAIRSVILLE				
Sample number	SC10	ST9	ST7	ST6
Color	dark grey, honey, medium grey	light grey, speckeled	black with blueish cast	medium grey
Relict rock type	mudstone; chert	biomicrite, chertified; chert	biomicrite, chertified; micrite	micrite
Structure				
lamination	1	0	1	0
cross bedding	0	0	0	0
graded	0	0	0	0
bioturbation	1	1	0	1
wavy lamination	0	0	0	0
convoluted bedding	0	0	0	0
Fossils				
detail preserved	0	0	1	0
ghosts	1	0	1	0
replaced	1	1	1	1
sponge spicules	1	0	0	0
poor preservation	0	?	0	0
Carbonate				
rhombs	0	0	1	0
grains	0	0	0	0
Hematite	0	1	0	0
Pyrite				
crystallites	0	1	0	0
disseminated	1	1	1	0
ghosts	0	0	0	0
massive	0	0	0	0
Organic Matter	0	1	0	0
Silica				
opaque	1	1	0	0
clear	0	0	0	0
grains	0	0	0	0
Stylolites	1	0	0	0

ST. CLAIRSVILLE					
Sample number	ST5	ST4	ST3	ST2	ST1
Color	medium grey, buff	medium grey	medium grey	medium-dark grey	brown; white
Relict rock type	biomicrite, chertified	biomicrite,	packed biomicrite; chertified	micrite; micrite, chertified	micrite; chert
Structure					
lamination	0	1	1?	0	0
cross bedding	0	0	0	0	0
graded	0	0	0	0	0
bioturbation	1	1	0	1	1
wavy lamination	0	0	0	0	0
convoluted bedding	0	0	0	0	0
Fossils					
detail preserved	1	0	1	0	1
ghosts	1	0	1	1	1
replaced	1	1	1	1	1
sponge spicules	0	0	1	0	0
poor preservation	1	0	1	1	1
Carbonate					
rhombs	1	0	0	0	0
grains	0	0	0	0	0
Hematite	1	1	1	0	0
Pyrite					
crystallites	0	0	0	0	0
disseminated	0	1	0	0	1
ghosts	1	1	0	1	1
massive	0	0	1	0	0
Organic Matter	1	1	?	1	1
Silica					
opaque	1	0	1	1	1
clear	1	0	0	1	1
grains	1?	0	0	0	0
Stylolites	1	1	1	0	0

TYRONE					
Sample number	T4	T3	T2		
Color	blue-grey	blue-grey	blue-grey		
Relict rock type					
Structure					
lamination	1	0	0		
cross bedding	0	0	0		
graded	0	0	0		
bioturbation	0	1	1		
wavy lamination	0	0	0		
convoluted bedding	0	0	0		
Fossils					
detail preserved		0	0		
ghosts	1	1	0		
replaced	1	1	0		
sponge spicules	0	0	0		
poor preservation	1	0	1		
Carbonate					
rhombs	0	0	1		
grains	0	0			
Hematite	0	1	1		
Pyrite					
crystallites	0	0	0		
disseminated	0	0	0		
ghosts	0	1	0		
massive	0	0	0		
Organic Matter	1	0	1		
Silica cement					
opaque	0	0	0		
clear	0	1	0		
grains	0	0	0		
Stylolites	0	0	0		

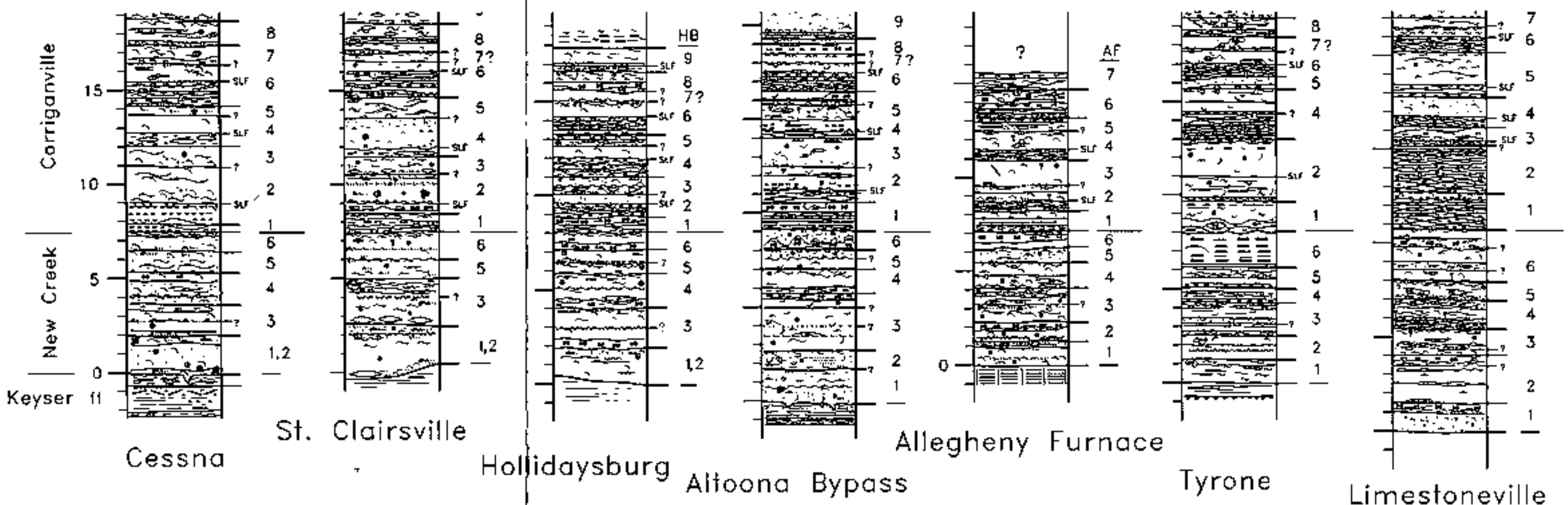

Plate 1. Correlated columnar sections, from Cessna to Limestoneville.